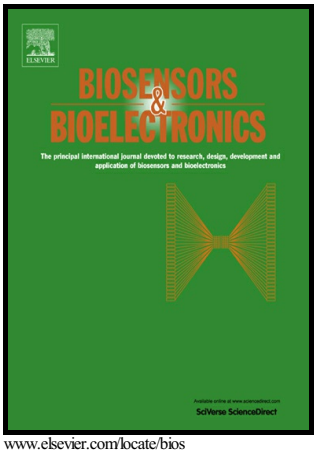

www.elsevier.com/locate/bios

RuO_2/graphene nanoribbon composite supported on screen printed electrode with enhanced electrocatalytic performances toward ethanol and NADH biosensing

Vesna Vukojević, Sladjana Djurdjić, Miloš Ognjanović, Bratislav Antić, Kurt Kalcher, Jelena Mutić, Dalibor M. Stanković

PII: S0956-5663(18)30468-8
DOI: https://doi.org/10.1016/j.bios.2018.06.038
Reference: BIOS10558

To appear in: *Biosensors and Bioelectronic*

Received date: 11 April 2018
Revised date: 5 June 2018
Accepted date: 20 June 2018

Cite this article as: Vesna Vukojević, Sladjana Djurdjić, Miloš Ognjanović, Bratislav Antić, Kurt Kalcher, Jelena Mutić and Dalibor M. Stanković, RuO_2/graphene nanoribbon composite supported on screen printed electrode with enhanced electrocatalytic performances toward ethanol and NADH biosensing, *Biosensors and Bioelectronic,* https://doi.org/10.1016/j.bios.2018.06.038

RuO_2/graphene nanoribbon composite supported on screen printed electrode with enhanced electrocatalytic performances toward ethanol and NADH biosensing

Vesna Vukojević[1*], Sladjana Djurdjić[2], Miloš Ognjanović[3], Bratislav Antić[3], Kurt Kalcher[4], Jelena Mutić[2], Dalibor M. Stanković[1,3*]

[1] *Innovation Center of the Faculty of Chemistry, University of Belgrade, Studentski Trg 12-16, 11000 Belgrade, Serbia*

[2] *Faculty of Chemistry, University of Belgrade, Studentski Trg 12-16, 11000 Belgrade, Serbia*

[3] *The Vinca Institute of Nuclear Sciences, University of Belgrade, POB 522, 11001 Belgrade, Serbia*

[4] *Institute of Chemistry-Analytical Chemistry, Karl-Franzens University Graz, A-8010 Graz, Austria*

*corresponding authors: Vesna Vukojević, Innovation center of the Faculty of Chemistry, University of Belgrade, Studentski Trg 12-16, 11000 Belgrade, Serbia. Email: vvukojevic@chem.bg.ac.rs Phone: 00381 11 3336829

Dalibor M. Stanković, The Vinca Institute of Nuclear Sciences, University of Belgrade, POB 522, 11001 Belgrade, Serbia. Emails: dalibors@chem.bg.ac.rs daliborstankovic@vin.bg.ac.rs Phone: 00381 11 3336829

Abstract

In this work, we aimed to propose a newly synthesized composite material with enhanced electrocatalytic properties as a novel screen-printed sensor for the quantification of NADH. Additionally, the surface was modified with alcohol dehydrogenase for the preparation of an amperometric biosensor for analysis of ethanol. Synthesized material was characterized using several microstructural (FE-SEM, HR-TEM, XRD) and electrochemical (CV, EIS) techniques. The electrochemical response of the tested analytes was investigated as a function of important parameters. Under optimal conditions, the working linear range and limit of detection for ethanol sensing was 1 to 1800 μM and 0.19 μM, respectively. For NADH, the linear range was from 1 to

1300 µM with limit of detection of 0.52 µM. Moreover, effects of some possible interfering compounds were investigated and the developed procedure was applied to commercial alcoholic beverages. The results obtained showed satisfactory precision and accuracy of the developed method and confirm the proposed approach could be a possible replacement for the currently used techniques for ethanol and NADH quantification.

Keywords: ethanol biosensor; screen printed electrode; graphene nanoribbons; alcohol dehydrogenase.

1. Introduction

In the last few decades, significant efforts have been made to develop various biosensors for the detection of numerous biological compounds such as ethanol, glucose, and amino acids (Maduraiveeran et al. 2018). Although many of these compounds can be quantified using several methods, including chromatography and spectrophotometry, the greatest effort has been dedicated to electrochemical biosensors. Alcohol, after water and tea, is the third most common beverage in the world (Cinti et al. 2017). Accurate and precise analysis of ethanol is of great importance in various applications, from industrial and food process control to clinical requirements (Bilgi et al. 2018). The significance of the coenzyme nicotinamide adenine dinucleotide (NADH) is related to the cellular respiration redox reaction. Conversion of NADH to NAD^+ can be by a huge number of dehydrogenases with different biocatalytic activities (Li et al. 2013). Therefore, the existence of selective and sensitive methods for monitoring this enzymatic process is of great importance. Electrochemical biosensors are preferable in monitoring enzyme reactions due to their low-cost, ease of manipulation, relatively fast response times and small size (Gupta et al. 2018).

The relatively recent development of screen printing technology has found wide application in the field of electrochemistry, offering sensitive, miniaturized and portable sensors and a basis for the development of biosensors. These electrodes are usually working electrodes prepared from conductive inks based on platinum, silver, copper or carbon. These versatile and cheap electrodes have overcome the main disadvantages of commercial electrodes and have attracted considerable attention in practically all fields of chemistry (González-Sánchez et al. 2018).

Carbon- and metal-based nanomaterials are increasingly used in the development of new biosensors due to their high surface area and biocompatibility (Aydoğdu Tığ 2017; Wang 2008). Carbon is one of the most commonly used materials in electroanalysis. Carbon nanomaterials, such as single- or multi-walled carbon nanotubes, graphene and recently, graphene nanoribbons (GNRs) are very popular in biosensing, as they have several desirable properties, such as high surface area, acceptable biocompatibility, chemical and electrochemical stability and good electrical conductivity (Eguílaz et al. 2016; Kuo et al. 2018; Lawal 2018; Shao et al. 2010; Wang 2008; Wu et al. 2007). Different combinations of these materials can be used for constructing biosensors or microbiosensors. The detection of hydrogen peroxide, based on ultrathin concave Ag nanosheets, was reported (Ma et al. 2018), while hydrogen peroxide sensing based on graphene blended with SnO_2 and Pd-Pt nanocages has been proposed (Fu et al. 2018). Glutathione detection using ZnO nanorod arrays synthesized on reduced graphene oxide was reported (Kang et al. 2015), while a microbiosensor for glucose was constructed based on single-stranded DNA functionalized single-walled carbon nanotubes (Kang et al. 2014). Also, several composite materials were employed for the construction of NADH or ethanol biosensors. The synergetic effect of pyrroloquinolone quinone and graphene nano-interface for NADH sensing was studied (Han et al. 2017). A composite of gold nanoparticles on electrochemically reduced graphene oxide, stabilized with poly(allylamine hydrochloride was used for NADH sensing (Istrate et al. 2016), while a similar approach was proposed for NADH sensing in urine (Govindhan et al. 2015). Ethanol sensing was proposed by several research groups using different modifiers and different platforms. Ethanol quantification has been recorded using a paper-based nanomodified sensor (Cinti et al. 2017), using palladium-modified graphene as a nanocomposite (Kumar et al. 2016), and using an ethanol biosensor based on a MnOx-MoOx electrode decorated with platinum nanoparticles (Ozdokur et al. 2016). An interesting approach was developed for simultaneous monitoring of ethanol and glucose using a bienzymatic biosensor based on gold nanoparticles decorated on a core-shell Fe_3O_4- and MnO_2-modified carbon paste electrode (Samphao et al. 2018). On the other hand, several research groups developed simultaneous detection of ethanol and NADH using different approaches. A rosmarinic acid-modified screen printed carbon electrode (SCPE) was proposed (Bilgi et al. 2018), as was a graphene/gold nanorod composite-based determination (Li et al. 2013; Wu et al. 2007) using carbon nanofibers (Wu et al. 2007), and gold-silver nanoparticles with poly(L-

cysteine)/reduced graphene nanocomposite was also used (Aydoğdu Tığ 2017). GNRs are one-dimensional strips of graphene (Mehmeti et al. 2017) and can be produced with desired characteristics, width and length. Due to this, GNRs have found wide application in the fields of micro- and nanoelectronics, physics, and recently, in the area of electrochemical biosensors (Mehmeti et al. 2017). Easy functionalization of GNRs, where novel functionalization moieties can be located at the edges of GNR strips, can increase important characteristics, such as electrostatic interaction, hydrogen bonding or covalent interactions (Martín et al. 2014).

Herein, we describe a disposable electrochemical biosensor for simultaneous detection of NADH and ethanol using modified screen-printed carbon electrodes (SPCEs). We report, for the first time, the electrocatalytic oxidation of NADH by a graphene nanoribbon-ruthenium dioxide/ screen-printed carbon electrode (GNR-RuO_2/SPCE). We also utilize the resulting electrode for development of a new ethanol biosensor through the immobilization of alcohol dehydrogenase (ADH). According to the best of our knowledge, there are no papers published on GNRs used for the preparation of biosensors for the detection of NADH or ethanol.

2. Experimental

All electrochemical measurements (cyclic voltammetry and chronoamperometric) were performed using a potentiostat/galvanostat Autolab PGSTAT 302N (MetrohmAutolab B.V., The Netherlands) controlled by software Nova 2.0. Electrochemical measurements were conducted in three electrode glass cells (total volume of 25 ml) with an Ag/AgCl electrode (3 M KCl) as reference electrode and Pt wire as counter electrode. Each potential reported in this paper is given against the Ag/AgCl/3M KCl electrode at ambient temperature (25+1°C). For pH measurements, a pH meter, model Orion 1230 equipped with a combined glass electrode model Orion 9165BNWP (USA), was used.

Microstructure and morphology of synthesized materials were investigated using a field emission-scanning electron microscope FE-SEM MIRA3 (Tescan, Czech Republic) coupled with an EDS analyser (Oxford, UK) operating at 30 kV. High-resolution transmission electron microscopic (HR-TEM) images were taken using transmission electron microscope (FEI, Talos F200X, Thermo Fisher Scientific, US) at an accelerating voltage of 200 kV. Diluted dispersions

of RuO_2, GNR and RuO_2-GNR nanocomposites were dropped on a carbon-coated copper grid and left to dry at room temperature for FE-SEM and HR-TEM observations. Images were analysed by Image J (Schneider et al. 2012) software in manual mode. The mean particle size was obtained by measuring the average diameter of total 200 particles using images collected in different parts of the grid. The nanoparticle size distributions were fitted through Origin software using the log-normal function, $y = y_0 + \frac{A}{\sqrt{2\pi\omega x}} \exp \frac{-\left[\ln\frac{x}{x_c}\right]^2}{2\omega^2}$.

Crystallographic properties were examined by X-ray powder-diffraction (XRD) performed on a high-resolution SmartLab® X-ray diffractometer (Rigaku, Japan) with Cu Kα radiation source (λ = 1.54056 Å), an accelerating voltage of 40 kV and current 30 mA. Samples were prepared by pressing dried powders on a zero-background silicon wafer, and diffraction patterns were collected within 15-70° 2θ range.

All chemicals were of analytical grade and were used as supplied, without any further purification. ADH (alcohol dehydrogenase from *Saccharomyces cerevisiae*), GNRs (length 2-15 μm, width 40-250 nm) and ruthenium (III) chloride hydrate used for synthesis of modified materials were obtained from Sigma Aldrich. NADH (dihydronicotinamide adenine dinucleotide disodium salt NADH-Na_2), potassium ferricyanide ($K_3[Fe(CN)_6]$), and potassium ferrocyanide ($K_4[Fe(CN)_6]$) were all supplied by Merck (Germany). All measurements were performed in 0.1 M phosphate buffer solution (PBS) (pH 7.50), which was obtained by dissolving corresponding amounts of phosphate salts (K_2HPO_4 and KH_2PO_4, Merck) in ultra-pure water. For preparation of standard solution of ethanol, 100 % absolute ethanol HPLC grade (ChemLab) was used.

2.1.Preparation of working electrodes

2.1.1. Preparation of SPCE electrodes

Thick layers of carbon ink (No. C50905DI, Gwent, Pontypool, UK) were applied to laser pre-etched ceramic supports (No. CLS 641000396R, Coors Ceramics GmbH, Chattanooga, TN, USA) by brushing the ink through an etched stencil (thickness 100 mm, electrode printing area 105 mm^2) with the aid of a screen printing device (SP-200, MPM, Franklin, MA, USA) onto the substrates. The resulting plates were dried overnight at room temperature to produce SPCEs.

2.1.2. Preparation of RuO_2-GNR/SPCE

In order to produce RuO_2-GNR/SPCE working electrodes, firstly we synthesized RuO_2/GNR composite, following the procedure described in the literature (Amir et al. 2015). Briefly, 5 mg of GNRs were suspended in 10 ml of ultrapure water and this mixture was sonicated for 1 hour. Then, 311 mg of $RuCl_3 \cdot xH_2O$ was added, with continuous stirring. Potassium hydroxide (0.1 M) was used during stirring in order to obtain pH 7 in the solution. After 12 h, the solution was centrifuged and washed three times with ultrapure water and once with ethanol. Prior to use, RuO_2-GNR composite was dried, dissolved in dimethylformamide (the concentration was 5 mg/ml) and sonicated for 3 hours. After this period, 5 µL of RuO_2/GNR composite were deposited on the prepared SPCE and allowed to dry at room temperature, to produce RuO_2-GNR/SPCE. This procedure was also performed without GNRs to produce RuO_2/SPCE, in order to compare electrochemical properties of the obtained materials.

2.1.3. Preparation of biosensor

For biosensor preparation, alcohol dehydrogenase (ADH) solution was prepared by dissolving 0.1 g of enzyme in 10 ml PBS buffer solution (pH 7.50). ADH solution was kept in the refrigerator until further use. ADH solution (5 µL) was added to RuO_2-GNR/SPCE and dried at 4 °C overnight. After this period, 2.5 µL of Nafion solution (5 % Nafion in ethanol) was dispersed on the electrode surface and allowed to dry at 4 °C to produce the biosensor.

3. Results and discussion

3.1.Characterization of working electrodes

Electrochemical characterization of four electrodes, SPCE, GNR/SPCE, RuO_2/SPCE and RuO_2-GNR/SPCE, was performed in 5 mM $[Fe(CN)_6]^{4-/3-}$ prepared in 0.1 M PBS (pH 7.50) at a scan rate of 50 mV/s. The voltammograms obtained are presented in Figure 1. As can be seen, with GNR/SPCE as the working electrode, absence of oxidation or reduction peaks was observed. In the case of all other examined electrodes, both peaks were present (Figure 1). Oxidation peaks appeared in the potential range from 0.55 up to 0.70 V and reduction peaks in the potential range from -0.15 to -0.3 V. However, the highest current and the best peak shape was obtained using RuO_2-GNR/SPCE, which confirmed that nanoparticles of RuO_2 in cooperation with GNRs significantly improved the characteristics of the bare screen printed electrode (Amir et al. 2015).

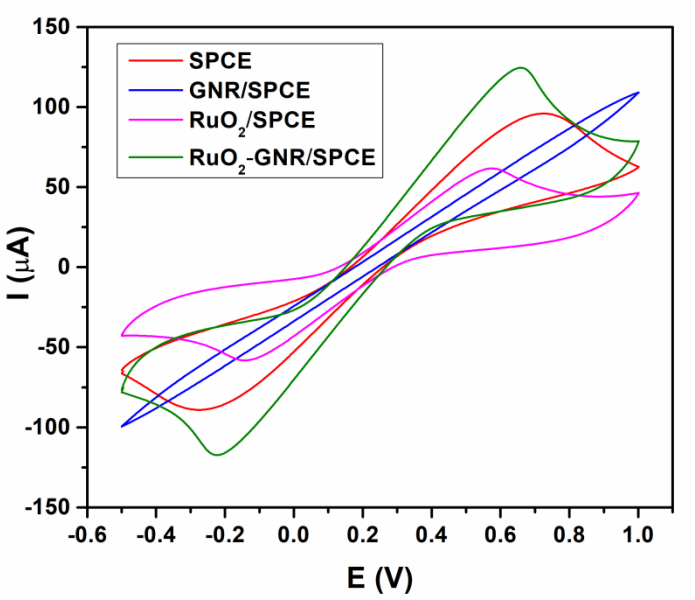

Figure 1. Cyclic voltammograms performed in 5 mM $[Fe(CN)_6]^{4-/3-}$ prepared in 0.1M phosphate buffer solution (pH 7.50) with SPCE, GNR/SPCE, RuO_2/SPCE and RuO_2-GNR/SPCE at a scan rate of 50 mV/s.

After confirmation that RuO_2-GNR/SPCE had the best response regarding the $[Fe(CN)_6]^{4-/3-}$ couple, the electrochemical response of all four electrodes to NADH was examined using cyclic voltammetry. Figure 2a displays cyclic voltammograms for the bare SPCE, GNR/SPCE, RuO_2/SPCE and RuO_2-GNR/SPCE in 0.1 M PBS with a scan rate of 50 mV/s in the presence of 1 mM NADH. The electro-oxidation peak of NADH using the bare SPCE was observed at +0.68 V in the potential range from -0.5 V to +1 V. For RuO_2/SPCE, no well-defined peak was observed. Meanwhile, for GNR/SPCE and RuO_2-GNR/SPCE, an obvious decrease in the peak potential and an increase in the current response were obtained in comparison with the bare SPCE peak (Figure 2a). The best peak shape was obtained for GNR/SPCE, but slightly higher current was achieved with RuO_2-GNR/SPCE. Additionally, the amperometric response of the electrodes toward addition of NADH was tested with all electrodes. Results are shown in Figure 2b. Similarly to our cyclic voltammetry results, the best analytical response was achieved with GNR/SPCE and RuO_2-GNR/SPCE. As can be seen, a better response was observed with RuO_2-GNR/SPCE, which produced more stable and reproducible signals. This could be connected with the involvement of RuO_2 nanoparticles in the structure of the composite and with the increased number of active surface sites.

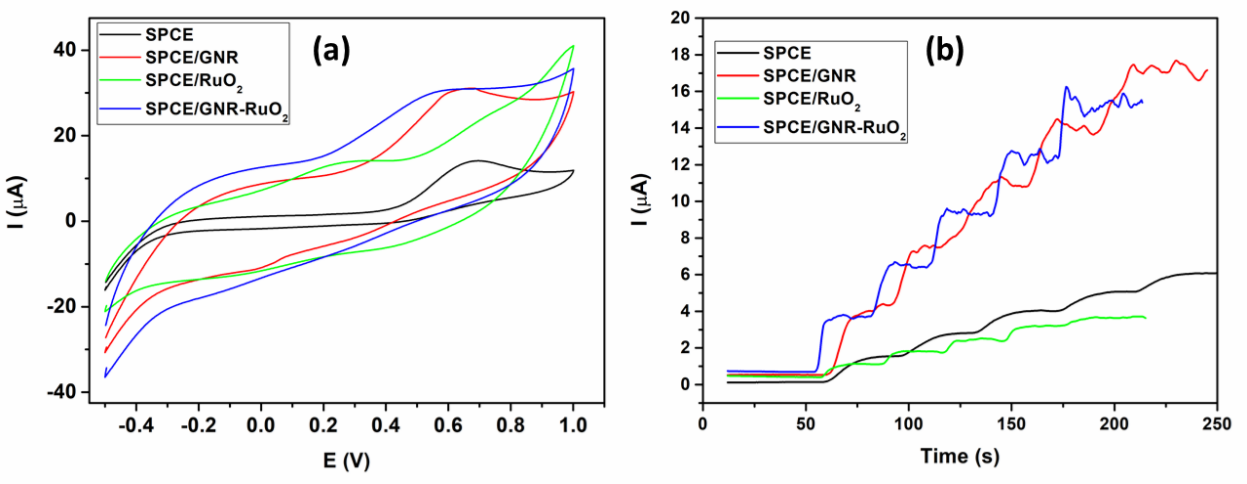

Figure 2. (a) Cyclic voltammograms performed in 0.1 M phosphate buffer solution (pH = 7.50) with SPCE, GNR/SPCE, RuO_2/SPCE and RuO_2-GNR/SPCE with addition of 1 mM NADH. Scan rate of 50 mV/s; (b) Chronoamperograms obtained for addition of 0.2 mmol NADH using all electrodes.

The morphology and surface structure of the RuO_2/GNR composite and its component materials were investigated by HR-TEM and FE-SEM. Figure 3a shows RuO_2 was composed of small pseudospherical log-normally distributed partially agglomerated nanoparticles at average diameter of ~2 nm enabling a high surface area (inset of Figure 3a). Figure 3b shows the morphology of GNRs, with long curved nanorods/nanotubes in addition to the granular and grain-like objects. The average width and length of GNRs was about 100 nm and a few micrometres, respectively. Small RuO_2 nanoparticles formed densely and homogeneously grown mats on top of the GNR support (Figure 3c), which can also be seen from EDS mapping (Supplementary material, Figure S1), significantly improving the surface area of the GNRs.

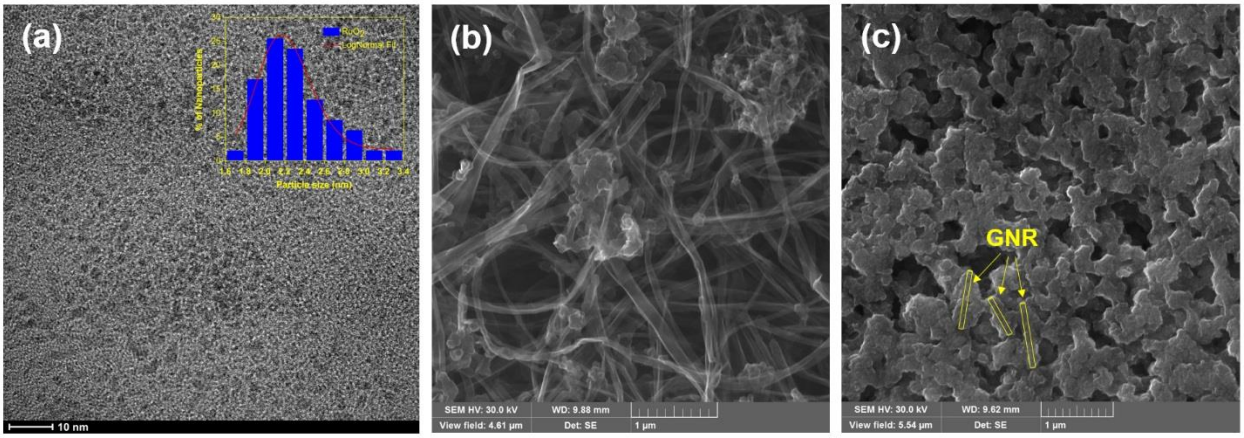

Figure 3. (a) HR-TEM micrograph of RuO_2 nanoparticles; FE-SEM micrographs of (b) GNR and (c) RuO2/GNR composite. Inset of Figure 3a shows log-normal size distribution of RuO_2 nanoparticles.

The microstructure of the obtained nanocrystals was tracked by XRD. Representative XRD patterns of GNRs and RuO_2/GNR composite and pure RuO_2 are shown in Figure S2. The pattern of GNRs (green line) shows a sharp diffraction peak at about $2\theta = 26.1°$, which can be attributed to the (002) plane of GNRs with interlayer d-spacing of 3.4 Å, which is in good agreement with graphene and CNTs (Liu et al. 2015). The sharp XRD peak indicates high crystallinity of GNRs, with crystal size of 26.6 nm, calculated using the Scherrer equation considering the (002) plane. Two small peaks at 2θ of 42.8° and 54.1° can be attributed to the (101) and (004) reflections of graphite. The two broad reflections of RuO_2/GNR composite (Figure S2, blue line) appeared at approximately the same positions as those of pure RuO_2 (red line), but the width and intensity indicate that the nanocomposite is not in pure crystalline form or the reason for the broad reflections could be due to the small particle size as seen from HR-TEM. Accordingly, the XRD pattern of the RuO_2/GNR composite suggests the material is a nanocomposite of highly dispersed RuO_2 on top of the GNRs.

3.2.Optimization of analytical parameters for RuO_2-GNR/SPCE

The effect of the operating potential on the current response of the RuO_2-GNR/SPCE was studied. Chronoamperometric responses and corresponding calibration curves of the NADH at different potentials are shown in Figure S3. As can be seen, at potential +0.2 V, satisfactory linearity as well as limit of detection (LOD) was obtained. However, very low current response was measured at +0.2 V, while a significant increase in oxidation peak current with the increase

of operating potential was noticed. Due to that, the potential of +0.6 V was chosen for the following measurements since the best analytical parameters were obtained for this potential (Supplementary material, Table S1).

The effect of different pHs on the response of the electrode for the detection of NADH was tested in the pH range from 6 to 8.5 in PBS using cyclic voltammetry. This pH range was selected based on the instability (i.e. degradation) of NADH at more alkaline and more acidic pHs outside this range (Bilgi et al. 2018). From the bar diagram (Supplementary material, Figure S4), it can be seen that the highest current was obtained at pH 7.5, and so this optimum pH was used for the detection of NADH using the proposed approach.

3.2.1. Amperometry of NADH, detected using the RuO_2-GNR/SPCE biosensor

Construction of the calibration curve for the quantification of NADH using RuO_2-GNR/SPCE biosensor was conducted under the previously optimized experimental conditions, pH 7.5 in PBS and at an operating potential of +0.6 V. At this selected potential, current was recorded as a function of time for different NADH concentrations. An amperogram and calibration curve are depicted in Figures 4a and b. A working linear range from 1 to 1300 µM with a LOD of 0.52 µM was obtained. LOD was calculated as $3\sigma_{intercept}$/slope. Linear regression equation was estimated as I(µA) = 0.40209 + 0.01031 C(µM) with regression coefficient of r = 0.99918. Relative standard deviation (RSD) was calculated for three different concentrations of NADH: 5, 100 and 500 µM, from a calibration curve, based on five measurements. The obtained RSD values of 5.4 %, 3.7 % and 2.9 %, for the concentrations 5, 100 and 500 µM, respectively, indicate satisfactory repeatability of the RuO_2-GNR/SPCE biosensor. Also, the lifetime of the electrode for NADH detection was tested using inter-day and intra-days studies. The biosensor did not lose more than 5 % of its activity during five days. The preparation pathway of the biosensor was tested by studying five independently prepared electrodes. The RSD value of 5.3 % confirmed the high reproducibility of the preparation procedure. All these results indicate good accuracy and satisfactory precision of the proposed biosensor and its production method.

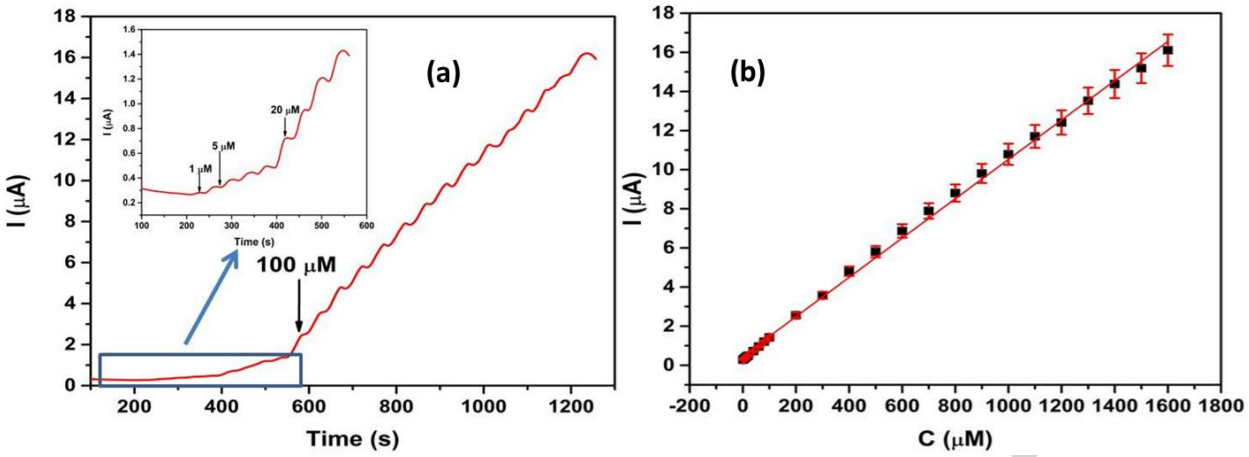

Figure 4. (a) Amperogram for the NADH quantification using RuO_2-GNR/SPCE biosensor at operating potential of 0.6 V in phosphate buffer solution at pH 7.5; (b) Corresponding calibration curve.

3.2.2. Amperometry of ethanol, detected using the RuO_2-GNR/SPCE biosensor

Analytical characteristics of the developed RuO2-GNR/SPCE biosensor were tested by recording its amperometric response after successive addition of known amounts of ethanol standard solution. Results are shown in Figures 5a and b. The linear working range for ethanol detection was found to be from 1 to 1800 μM with LOD of 0.19 μM. By comparing our results with similar biosensors found in the literature (Table 1), it can be concluded that the electrode developed in this work possesses one of the widest linear ranges and comparable or better LOD. The reproducibility of the biosensor's ability to detect ethanol was also examined. After one day of intensive usage to detect ethanol, changes in the signal current were not higher than 4 % at the end of the day. The electrode lost 8 % of activity at the start of the second day after overnight storage at 4 °C, and up to 65 % of activity after the fifth night of storage. Also, RSDs for 5, 50 and 100 μM ethanol (n = 5) were 4.7 %, 3.9 % and 3.1 %, respectively, suggesting excellent repeatability of the developed biosensor and ethanol detection method. Additionally, measurements of 20 μM ethanol using five independently prepared electrodes produced a RSD of 4.3 %, indicating excellent reproducibility of the biosensor and satisfactory accuracy and precision of the developed procedure.

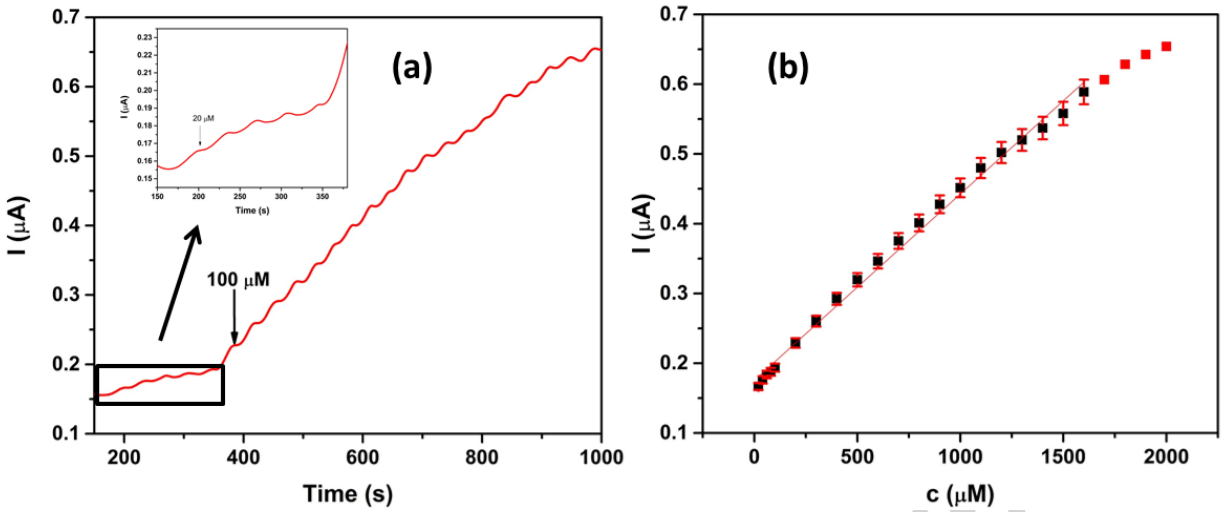

Figure 5. (a) Amperogram for the detection of ethanol using the developed biosensor at operating potential of 0.6 V in phosphate buffer solution at pH 7.5; (b) Corresponding calibration curve.

Table 1. Comparison of the recently reported literature ethanol biosensors

Electrode	Range (μM)	LOD (μM)	Sensitivity	Ref
GCE/Au-AgNPs/P(L-Cys)-ERGO/ADH/Naf[a]	17 - 1845	5	0.177 μA/mM	(Aydoğdu Tığ 2017)
SPCE/MWCNT/AuNP/PNR/ADH/GA[b]	320.2–1000.	96.1	0.49 μA/mM	(Bilgi and Ayranci 2016)
polystyrene sulfonate MWCNT – ADH/Naf/GC[c]	70 – 420	19	15.6 μA·/mM·cm^2	(Barhoumi et al. 2017)
GN–AuNRs–ADH/GC[d]	5-377	1.5	102 μA·/mM·cm^2	(Li et al. 2013)
RuO_2-GNR/SPCE/ADH/Naf[e]	1-1800	0.19	4.5 μA·/mM·cm^2	*The current study*

[a]glassy carbon electrode/gold-silver bimetallic nanoparticles/poly(L-Cysteine)-electrochemically reduced graphene oxide/alcohol dehydrogenase/nafion (GCE/Au-AgNPs/P(L-Cys)-ERGO/ADH/Naf)

[b]screen-printed carbon electrode/multiwalled carbon nanotubes/gold nanoparticles/polyneutral red/alcohol dehydrogenase/glutaraldehyde (SPCE/MWCNT/AuNP/PNR/ADH/GA)

[c]polystyrene sulfonate multiwalled carbon nanotubes- alcohol dehydrogenase/nafion/glassy carbon electrode (polystyrene sulfonate MWCNT –ADH/Naf/GC)

[d]graphene–gold nanorods- alcohol dehydrogenase/glassy carbon electrode (GN–AuNRs–ADH/GC)

[e]graphene nanoribbons-ruthenium dioxide/screen-printed carbon electrodes/alcohol dehydrogenase/nafion (GNR-RuO_2/SPCE/ADH/Naf)

3.2.3. Interferences

The selectivity of the developed RuO_2-GNR/SPCE biosensor for the determination of NADH and ethanol was tested using the interfering compounds glucose (Glu) and ascorbic acid (AA). The developed RuO_2-GNR/SPCE electrochemical sensor did register oxidation of both selected interfering compounds. A negligible, lower effect was noticed for NADH sensing (Supplementary material, Figure S5). This was probably due to the selected operating potential, at which the interfering compounds are easily oxidized. These results lead to the conclusion that this biosensor would not be suitable for use with blood serum samples, but it could be applied in the ethanol content quantification of alcoholic beverages.

3.2.4. Measurement of the ethanol content in commercial beverages

Practical application of the developed biosensor was tested by measuring the ethanol content of some alcoholic beverages. Three different commercially-produced Serbian schnapps, plum, apricot and pear, with respective declared ethanol contents of 45, 40 and 38 % (Supplementary material, Table S2), were used. As can be seen, excellent agreement between the results obtained with our new biosensor and the declared contents of ethanol was achieved. These results clearly indicate the proposed procedure with the novel biosensor could be successfully applied for the quantification of ethanol in alcoholic beverages.

4. Conclusion

In this work, a novel biosensor for the quantification of ethanol and NADH was demonstrated, based on a composite containing RuO_2 and GNRs, supported on a screen-printed electrode. This approach allowed increased communication and electron transfer between the electrode surface

and redox centres in the alcohol dehydrogenase enzyme. The concept presented has promising potential to be applied to other enzymatic biosensors and to preparation of miniaturized and disposable electrochemical biosensors.

5. Acknowledgements

This work was supported by MagBioVin project (FP7-ERAChairs-Pilot Call-2013, Grant agreement: 621375), by the Ministry of Education, Science and Technology, the Republic of Serbia (Project No. OI 172030), and CEEPUS CIII-CZ-0212-11-1718 network; Education of Modern Analytical and Bioanalytical Methods.

References

Amir, F.Z., Pham, V.H., Dickerson, J.H., 2015. RSC Adv. 5 (83), 67638–67645.

Aydoğdu Tığ, G., 2017. Talanta 175, 382–389.

Barhoumi, L., Istrate, O.-M., Rotariu, L., Ali, M.B., Bala, C., 2017. Analytical Letters 51 (3), 323–335.

Bilgi, M., Ayranci, E., 2016. Sensors and Actuators B: Chemical 237, 849–855.

Bilgi, M., Sahin, E.M., Ayranci, E., 2018. Journal of Electroanalytical Chemistry 813, 67–74.

Cinti, S., Basso, M., Moscone, D., Arduini, F., 2017. Analytica chimica acta 960, 123–130.

Eguílaz, M., Gutierrez, F., González-Domínguez, J.M., Martínez, M.T., Rivas, G., 2016. Biosensors & bioelectronics 86, 308–314.

Fu, Y., Di Huang, Li, C., Zou, L., Ye, B., 2018. Analytica chimica acta 1014, 10–18.

González-Sánchez, M.I., Gómez-Monedero, B., Agrisuelas, J., Iniesta, J., Valero, E., 2018. Electrochemistry Communications 91, 36–40.

Govindhan, M., Amiri, M., Chen, A., 2015. Biosensors & bioelectronics 66, 474–480.

Gupta, S., Murthy, C.N., Prabha, C.R., 2018. International journal of biological macromolecules 108, 687–703.

Han, S., Du, T., Jiang, H., Wang, X., 2017. Biosensors & bioelectronics 89 (Pt 1), 422–429.

Istrate, O.-M., Rotariu, L., Marinescu, V.E., Bala, C., 2016. Sensors and Actuators B: Chemical 223, 697–704.

Kang, Z., Gu, Y., Yan, X., Bai, Z., Liu, Y., Liu, S., Zhang, X., Zhang, Z., Zhang, X., Zhang, Y., 2015. Biosensors & bioelectronics 64, 499–504.

Kang, Z., Yan, X., Zhang, Y., Pan, J., Shi, J., Zhang, X., Liu, Y., Choi, J.H., Porterfield, D.M., 2014. ACS applied materials & interfaces 6 (6), 3784–3789.

Kumar, M.A., Patnaik, S.G., Lakshminarayanan, V., Ramamurthy, S.S., 2016. Analytical Letters 50 (2), 350–363.

Kuo, Y.-C., Lee, C.-K., Lin, C.-T., 2018. Biosensors & bioelectronics 103, 130–137.

Lawal, A.T., 2018. Biosensors & bioelectronics 106, 149–178.

Li, L., Lu, H., Deng, L., 2013. Talanta 113, 1–6.

Liu, M., Du, Y., Miao, Y.-E., Ding, Q., He, S., Tjiu, W.W., Pan, J., Liu, T., 2015. Nanoscale 7 (3), 1037–1046.

Ma, B., Kong, C., Hu, X., Liu, K., Huang, Q., Lv, J., Lu, W., Zhang, X., Yang, Z., Yang, S., 2018. Biosensors & bioelectronics 106, 29–36.

Maduraiveeran, G., Sasidharan, M., Ganesan, V., 2018. Biosensors and Bioelectronics 103, 113–129.

Martín, A., Hernández-Ferrer, J., Vázquez, L., Martínez, M.-T., Escarpa, A., 2014. RSC Adv 4 (1), 132–139.

Mehmeti, E., Stanković, D.M., Chaiyo, S., Zavasnik, J., Žagar, K., Kalcher, K., 2017. Microchimica Acta 184 (4), 1127–1134.

Ozdokur, K.V., Demir, B., Atman, E., Tatli, A.Y., Yilmaz, B., Demirkol, D.O., Kocak, S., Timur, S., Ertas, F.N., 2016. Sensors and Actuators B: Chemical 237, 291–297.

Samphao, A., Butmee, P., Saejueng, P., Pukahuta, C., Švorc, Ľ., Kalcher, K., 2018. Journal of Electroanalytical Chemistry 816, 179–188.

Schneider, C.A., Rasband, W.S., Eliceiri, K.W., 2012. Nat Methods 9 (7), 671–675.

Shao, Y., Wang, J., Wu, H., Liu, J., Aksay, I.A., Lin, Y., 2010. Electroanalysis 22 (10), 1027–1036.

Wang, J., 2008. Chemical reviews 108 (2), 814–825.

Wu, L., Zhang, X., Ju, H., 2007. Analytical chemistry 79 (2), 453–458.

Highlights

- Novel synthesized composite material with enhanced electrocatalytic properties was used as screen-printed sensor for the quantification of NADH.
- Electrode surface was modified with alcohol dehydrogenase for the preparation of amperometric biosensor for analysis of ethanol.
- Material was characterized using microstructural and electrochemical techniques.
- Excellent performances were achieved using suggested approach.